

pubs.acs.org/NanoLett Letter

# Screen-Printable Hexagonal Boron Nitride Ionogel Electrolytes for Mechanically Deformable Solid-State Lithium-Ion Batteries

Woo Jin Hyun, Cory M. Thomas, Lindsay E. Chaney, Ana Carolina Mazarin de Moraes, and Mark C. Hersam\*



Cite This: Nano Lett. 2022, 22, 5372-5378



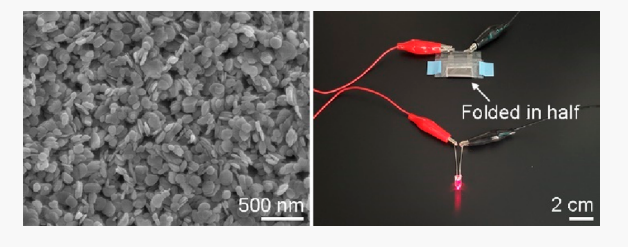
**ACCESS** 

III Metrics & More

Article Recommendations

s Supporting Information

**ABSTRACT:** Ionogel electrolytes present several benefits for solid-state lithium-ion batteries including nonflammability, favorable electrochemical properties, and high thermal stability. However, limited processing methods are currently available for ionogel electrolytes, restricting their practical applications. Here, we present a screen-printable ionogel electrolyte formulation based on hexagonal boron nitride (hBN) nanoplatelets. To achieve screen-printable rheological properties, hBN nanoplatelets are mixed with an imidazolium ionic liquid in ethyl lactate. Following screen printing, the resulting spatially uniform and



mechanically flexible hBN ionogel electrolytes achieve high room-temperature ionic conductivities >1 mS cm<sup>-1</sup> and stiff mechanical moduli >1 MPa. These hBN ionogel electrolytes enable the fabrication of fully screen-printed lithium-ion batteries with high cycling stability, rate performance, and mechanical resilience against flexion and external forces, thus providing a robust energy storage solution that is compatible with scalable additive manufacturing.

KEYWORDS: 2D materials, hBN nanoplatelet, ionic liquid gel, solid electrolyte, printed electronics, energy storage

onsiderable attention has recently been directed toward ✓ the development of solid-state electrolytes for lithium-ion batteries (LIBs). 1,2 Solid-state electrolytes address safety concerns of conventional liquid electrolytes by eliminating highly flammable carbonate solvents, allowing continuous advances in LIB energy density. Moreover, solid-state electrolytes remove leakage issues and thus significantly reduce packaging constraints, facilitating LIB production in a diverse range of battery form factors. However, currently available solidstate electrolytes based on inorganics and polymers face major challenges for practical applications, including low ionic conductivity, high interfacial resistance, and cumbersome processing based on unconventional equipment and environments for battery manufacturing. Ionogel electrolytes, which are composite electrolytes based on ionic liquids and gelling solid matrices, have attracted significant interest due to their potential to overcome these challenges.<sup>3,4</sup> In contrast to conventional liquid electrolytes, ionic liquids possess nonflammability, negligible vapor pressure, and high thermal stability. By blending ionic liquids with solid matrices, immobilization and gelation are induced, resulting in a mechanically flexible solid-state electrolyte. Ionogel electrolytes have been explored using a range of ionic liquids and solid matrices, achieving high ionic conductivity, wide electrochemical stability windows, favorable interfacial properties, and outstanding thermal stability. 5-9 However, the development of ionogel electrolytes has typically focused on electrolyte properties, whereas less attention has been paid to their processing methods for practical production

of LIBs, particularly using scalable additive manufacturing methods.

Printing processes offer significant benefits for LIB fabrication. 10,111 For example, printing processes enable additive manufacturing of LIBs, which minimizes materials waste and thus results in higher sustainability and lower costs of production when compared to traditional coating processes.<sup>12</sup> Moreover, printing processes are compatible with roll-to-roll production formats, which accelerate LIB production and consequently facilitate high-throughput manufacturing. To realize printable LIBs, various strategies have been explored, including inkjet, aerosol jet, screen, and three-dimensional printing 13-18 Among these printing methods, screen printing is particularly promising for LIB production due to its simplicity and scalability. Screen printing is an established printing method that deposits an ink through a screen mask composed of a mesh and patterned stencil. Screen-printable inks require optimized viscosities that are sufficiently low to allow the inks to pass through the screen mesh but also sufficiently high to minimize undesired ink spreading on the target substrate. 19 For screenprinted LIBs, various electrode and electrolyte materials have

Received: April 5, 2022 Revised: June 14, 2022 Published: June 21, 2022





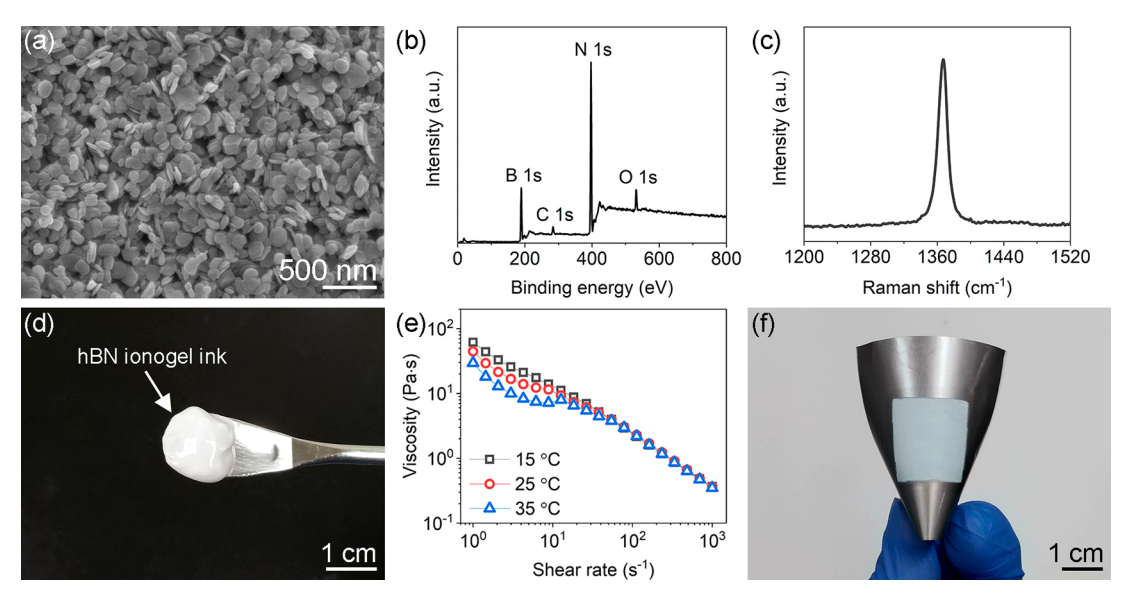


**Figure 1.** Screen-printable hexagonal boron nitride (hBN) ionogel electrolytes. (a) Scanning electron microscopy image of hBN nanoplatelets used as the gelling matrix for the ionogel electrolytes. (b) X-ray photoelectron spectroscopy and (c) Raman spectra of the hBN nanoplatelets. (d) Photograph and (e) shear viscosity of the screen-printable hBN ionogel electrolyte ink. (f) Photograph of the screen-printed hBN ionogel electrolyte in a 2 × 2 cm square pattern on an aluminum substrate.

been pursued, <sup>20–25</sup> but screen-printable ionogel electrolytes have not yet been realized.

Here, we report the development of screen-printable ionogel electrolytes using exfoliated hexagonal boron nitride (hBN) nanoplatelets as the gelling matrix. In addition to hBN being electrically insulating, chemically inert, thermally stable, and mechanically robust, the nanoscale size and large surface area of exfoliated hBN enable strong immobilization of ionic liquids without significant disruption of ion conduction pathways, yielding hBN ionogel electrolytes with high mechanical strength and ionic conductivity. 26 Screen-printable hBN ionogel electrolyte inks are prepared by dispersing hBN nanoplatelets and an imidazolium ionic liquid in ethyl lactate, enabling optimized viscosities for screen printing of spatially uniform and mechanically flexible solid-state electrolytes. Employing these hBN ionogel electrolyte inks, solid-state LIBs are screen-printed with LiFePO<sub>4</sub> (LFP) cathodes and Li<sub>4</sub>Ti<sub>5</sub>O<sub>12</sub> (LTO) anodes, exhibiting high rate performance and excellent cycling stability. Moreover, mechanical testing of the resulting screen-printed LIBs reveals outstanding stability against bending deformation and external forces, thus illustrating their suitability for mechanically flexible applications.

The hBN ionogel electrolytes are based on exfoliated hBN nanoplatelets (Figure 1a) and 1-ethyl-3-methylimidazolium bis(trifluoromethylsulfonyl)imide (EMIM-TFSI) ionic liquids containing 1 M lithium bis(trifluoromethylsulfonyl)imide (LiTFSI) salt. The hBN nanoplatelets were obtained from bulk hBN microparticles using a previously reported solutionbased exfoliation method.<sup>26</sup> Briefly, bulk hBN microparticles were shear-mixed with ethyl cellulose (EC) and ethanol, and exfoliated hBN/EC were collected by flocculation and centrifugation. After EC was removed by annealing at 400 °C, hBN nanoplatelets were obtained to prepare the hBN ionogel electrolytes (see the Methods section in the Supporting Information for more details). Figure 1b shows a survey X-ray photoelectron spectroscopy (XPS) spectrum, where the B 1s and N 1s peaks of the hBN nanoplatelets are evident at 189 and 397 eV, respectively. 27,28 Additional low-intensity XPS peaks are

observed for C 1s and O 1s because oxidized carbonaceous residues remain on the surface of the hBN nanoplatelets following pyrolysis of the stabilizing polymers used for the solution-based exfoliation method. These oxidized carbonaceous residues facilitate strong chemical interactions between the hBN nanoplatelets and the EMIM-TFSI ionic liquid, thus promoting strong gelation. Figure 1c displays a Raman spectrum of the hBN nanoplatelets with a characteristic peak at 1368 cm $^{-1}$ , which is assigned to the B-N vibrational (E $_{2g}$ ) mode, as expected for hBN.  $^{29,30}$ 

To formulate screen-printable inks, the hBN nanoplatelets and EMIM-TFSI/1 M LiTFSI were mixed with ethyl lactate in a glass bottle, and the solution was agitated with a magnetic bar. The ratio of the hBN nanoplatelets and EMIM-TFSI/1 M LiTFSI was 1:2 by weight, and the concentration of the hBN ionogel (i.e., hBN nanoplatelets and ionic liquid) in ethyl lactate was 750 mg mL $^{-1}$ . Figure 1d shows a photograph of the hBN ionogel electrolyte ink. The ink viscosity (Figure 1e) was measured to be 10 Pa s at a shear rate of 10 s $^{-1}$  at 25 °C without a significant temperature dependence for  $\pm 10$  °C. Furthermore, the ink presented a shear thinning behavior with a power law index (n) of 0.35 and a consistency index (K) of 44 Pa s, according to the Ostwald-de Wæle model

$$\mu = K \gamma^{n-1}$$

where  $\mu$  and  $\gamma$  are the ink viscosity and shear rate, respectively. Shear thinning rheological properties are desirable for screen-printable inks because the decreased viscosity at high shear rates eases ink penetration through the screen mesh during the screen printing process. <sup>31,32</sup>

After screen printing, the substrates were annealed at  $160\,^{\circ}$ C for 30 min to remove ethyl lactate, generating spatially uniform and mechanically flexible hBN ionogel electrolytes, as shown in Figure 1f. The storage modulus (G') of the hBN ionogel electrolytes was higher than the loss modulus (G'') with limited frequency and temperature dependence (Figure S1, Supporting Information), revealing reliable solid-like behavior. The hBN ionogel electrolytes also simultaneously exhibited desirable

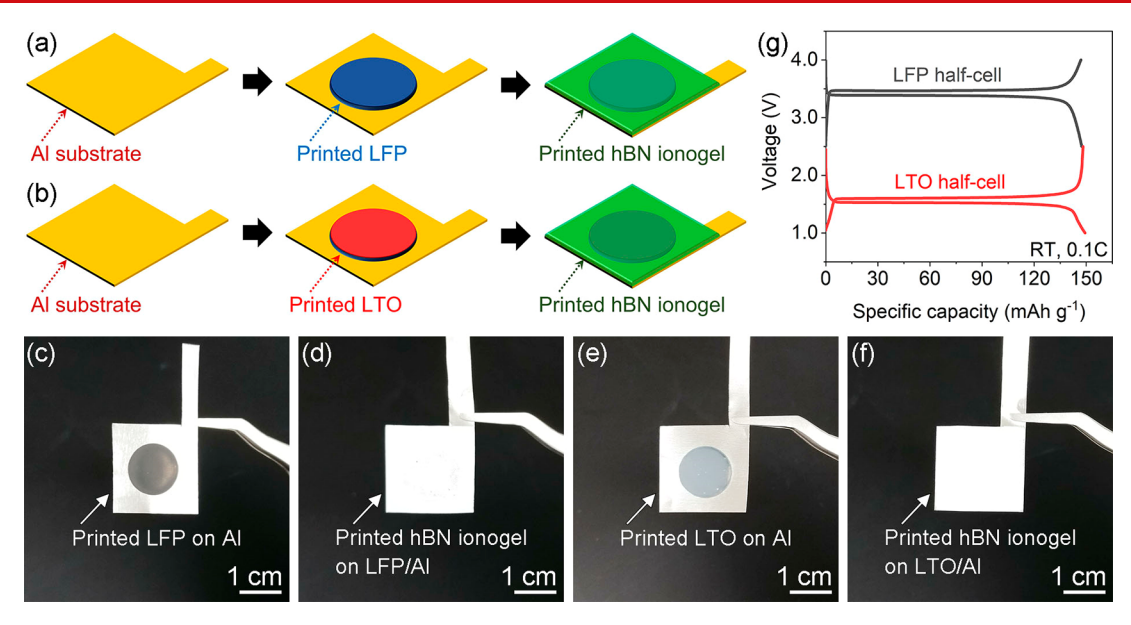
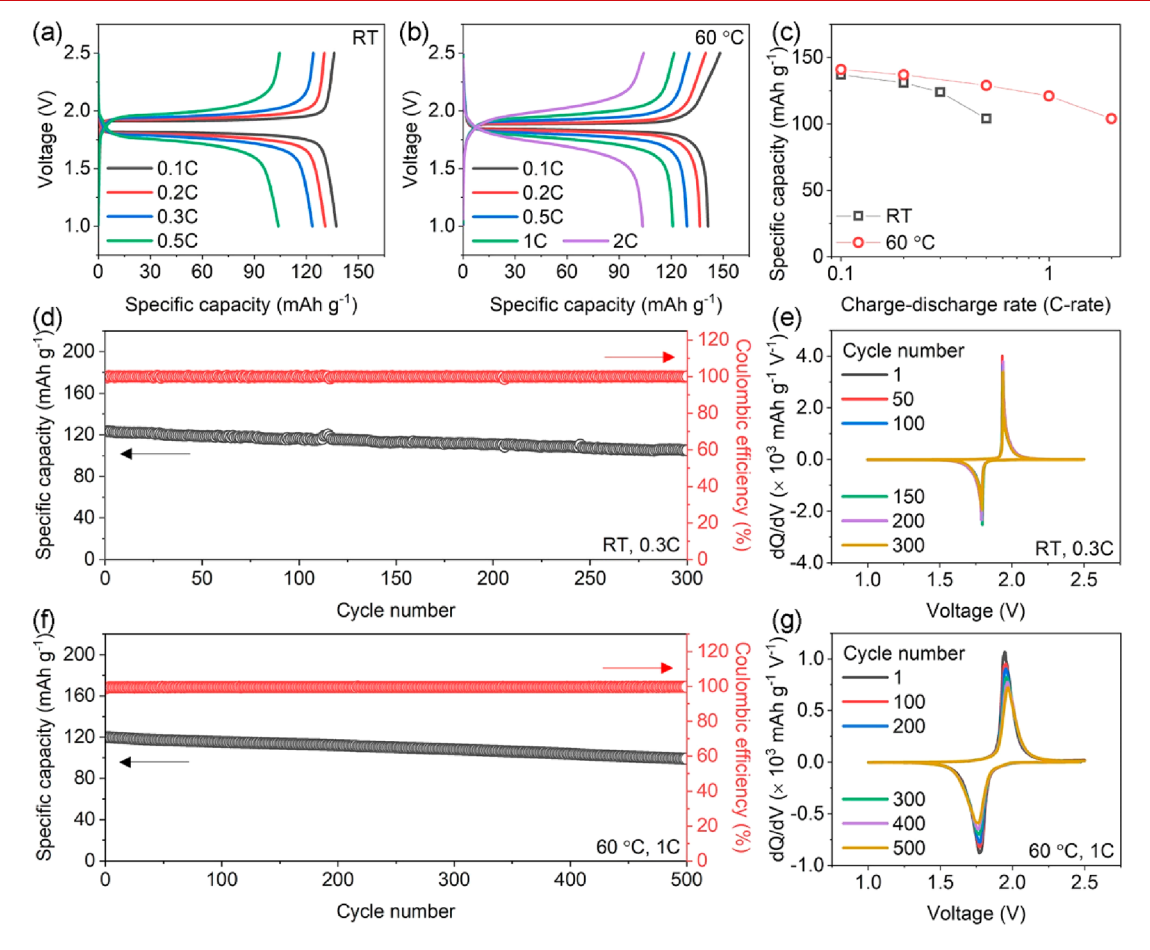


Figure 2. Screen-printed electrodes and electrolytes. (a) Schematic diagram for printing a LiFePO $_4$  (LFP) cathode and the hBN ionogel electrolyte on an aluminum substrate. (b) Schematic diagram for printing a Li $_4$ Ti $_5$ O $_{12}$  (LTO) anode and the hBN ionogel electrolyte on an aluminum substrate. Photographs of an aluminum substrate after printing the (c) LFP cathode and (d) hBN ionogel electrolyte. Photographs of an aluminum substrate after printing the (e) LTO anode and (f) hBN ionogel electrolyte. (g) Charge—discharge voltage profiles of half-cells using the printed LFP/hBN ionogel and LTO/hBN ionogel. The half-cells were measured at room temperature (RT) with a charge—discharge rate of 0.1C.



**Figure 3.** Electrochemical performance of screen-printed LFP/LTO full-cells using the hBN ionogel electrolytes. Charge—discharge voltage profiles at (a) room temperature and (b) 60 °C. (c) Comparison of the rate capability at room temperature and 60 °C. (d) Cycling performance and (e) differential capacity (dQ/dV) curves at room temperature with a charge—discharge rate of 0.3C. (f) Cycling performance and (g) differential capacity curves at 60 °C with a charge—discharge rate of 1C.

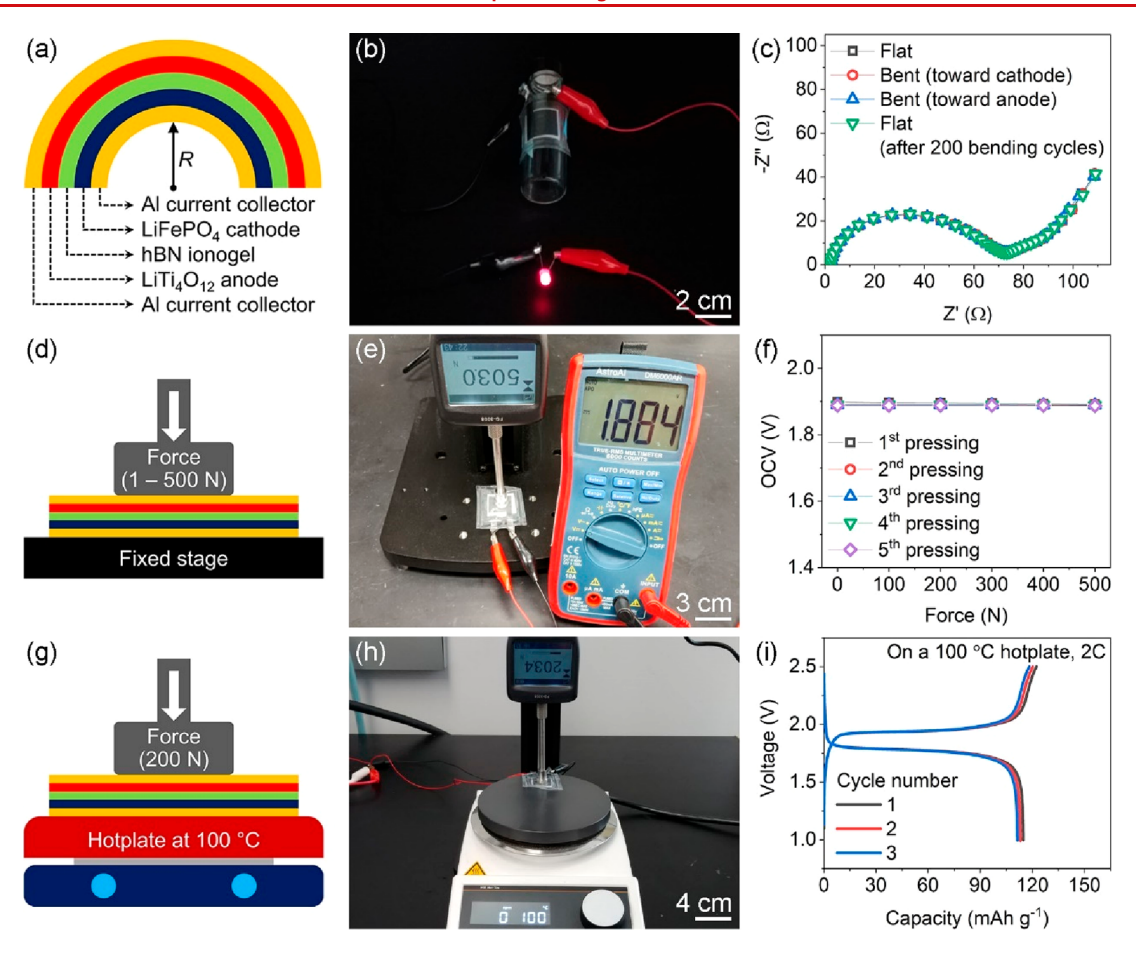


Figure 4. Mechanical deformation testing of screen-printed LFP/LTO full-cells using the hBN ionogel electrolytes. (a) Schematic for bending toward the cathode. (b) Photograph of the screen-printed LIB powering a light-emitting diode during bending. (c) Nyquist plots of the screen-printed LIB before/during bending and after 200 bending cycles. The 200 bending cycles include 100 bending cycles toward the cathode and 100 bending cycles toward the anode, with a bending radius (R) of 14 mm. (d) Schematic for pressing the battery. (e) Photograph of the screen-printed LIB while being pressed with a force over 500 N, showing an open-circuit voltage (OCV) of 1.884 V. (f) OCV of the screen-printed LIB while being pressed with forces ranging from 0 to 500 N five times. (g) Schematic for pressing the screen-printed LIB on a hot plate. (h) Photograph and (i) charge—discharge voltage profiles of the screen-printed LIB while being compressed with a force over 200 N on a hot plate at 100 °C.

mechanical moduli (G') exceeding 1 MPa and high ionic conductivities exceeding 1 mS cm<sup>-1</sup> at room temperature (Figure S2, Supporting Information), which can be attributed to the nanostructured hBN solid matrix. The exfoliated hBN nanoplatelets provide a large surface area to promote interactions with the ionic liquid for stronger gelation, enhancing the mechanical strength of the hBN ionogel electrolytes. In addition, their nanoscale size minimizes disruption of ion conduction pathways, allowing mechanical property enhancement without compromising ionic conductivity. Hence, while traditional ionogel electrolytes have shown a trade-off between their mechanical strength and ionic conductivity, the exfoliated hBN nanoplatelets enable the fabrication of ionogel electrolytes that possess concurrently high mechanical moduli and ionic conductivities.  $^{26}$ 

Figure 2a,b depicts the screen printing fabrication process for solid-state LIBs using the hBN ionogel electrolytes. On an aluminum substrate, LFP (Figure 2c) is first screen-printed as the cathode, and then, the hBN ionogel electrolyte (Figure 2d) is screen-printed on top of the cathode. On another aluminum substrate, LTO (Figure 2e) is first screen-printed as the anode, and then, the hBN ionogel electrolyte (Figure 2f) is screen-printed on top of the anode. The LFP and LTO inks (Figure S3, Supporting Information) were prepared with the active

materials, carbon black and poly(vinylidene fluoride) in a weight ratio of 8:1:1, employing 1-methyl-2-pyrrolidinone as a solvent. The LFP and LTO electrodes were deposited in a circular pattern with a diameter of 1.2 cm, and their loading was 5 mg cm<sup>-2</sup>. The thickness of the hBN ionogel electrolytes on both the cathode and anode was 15  $\mu$ m, which was sufficiently thick to uniformly cover the microporous electrodes (Figure 2d,f). In addition, while the electrodes were printed in air, the hBN ionogel electrolytes were printed in an argon-filled glovebox to minimize air exposure. Prior to the fabrication of LIB full-cells, LIB half-cells based on the screen-printed LFP/ hBN ionogel and LTO/hBN ionogel samples were tested to evaluate the lithium-ion capacity of the screen-printed electrodes in combination with the screen-printed hBN ionogel electrolytes. As shown in Figure 2g, the specific discharge capacities were measured to be 147 and 149 mAh  $g^{-1}$  at 0.1C for the LFP and LTO half-cells, respectively. Furthermore, both the LFP and LTO half-cells exhibited typical charge-discharge voltage profiles with well-defined plateaus, revealing the effective electrochemical operation of the screen-printed electrodes and electrolytes.

LFP/LTO full-cells were fabricated by sandwiching the screen-printed LFP/ionogel and LTO/ionogel (Figure S4, Supporting Information). Figure 3a,b displays the charge—

Nano Letters pubs.acs.org/NanoLett Letter

discharge voltage profiles of the LFP/LTO full-cells measured at room temperature and 60 °C, respectively, with various charge—discharge rates. At room temperature, the specific discharge capacity of the LFP/LTO full-cell was 137 mAh g $^{-1}$  at 0.1C, which remained higher than 100 mAh g $^{-1}$  at rates up to 0.5C. This favorable rate performance for a solid-state LIB can be attributed to the high room-temperature ionic conductivity of the hBN ionogel electrolytes. In addition, the specific discharge capacity at 60 °C was 141 mAh g $^{-1}$  at 0.1C, which remained higher than 100 mAh g $^{-1}$  at rates up to 2C. The improved rate capability at 60 °C compared to room temperature (Figure 3c) originates from the improved ionic conductivity of the hBN ionogel electrolytes at elevated temperatures (Figure S2, Supporting Information).

The cycling performance of the screen-printed LFP/LTO full-cells was also evaluated at room temperature and 60 °C. Figure 3d displays the specific discharge capacity and Coulombic efficiency for 300 cycles at 0.3C at room temperature (Figure S5, Supporting Information). The initial discharge capacity was 124 mAh g<sup>-1</sup>, and >85% of the initial capacity was retained after 300 cycles, which is equivalent to a capacity loss of less than 0.05% per cycle. In addition, the average Coulombic efficiency for the 300 cycles exceeded 99.9%. Figure 3e shows differential capacity curves of the printed LFP/LTO battery up to 300 cycles, where the peaks at 1.94 and 1.74 V are associated with the voltage plateaus for charging and discharging, respectively. The two major peaks showed minimal shifting during the cycling test, implying negligible changes in the LIB operating voltage and providing additional evidence of the outstanding cycling stability of screen-printed LIBs based on hBN ionogel electrolytes. Moreover, Figure 3f presents the specific discharge capacity and Coulombic efficiency of the screen-printed LFP/LTO full-cell for 500 cycles at 60 °C and a 1C rate (Figure S6, Supporting Information). The initial discharge capacity was 120 mAh g<sup>-1</sup>, and >82% of the initial capacity was retained after 500 cycles, which is equivalent to a capacity loss of less than 0.04% per cycle. In addition, the average Coulombic efficiency for this 500 cycle test exceeded 99.5%. Similar to the room-temperature results, the differential capacity curves at 60 °C (Figure 3g) presented minimal peak shifting for both the charging and discharging processes. Overall, the electrochemical characterization showed excellent cycling stability of the screen-printed LIBs both at room temperature and at elevated temperatures.

Table S1 (Supporting Information) compares the electrochemical performance of the screen-printed LFP/LTO full-cells based on the hBN ionogel electrolyte with literature precedent, revealing superior performance compared to previous printed LIBs using LFP and LTO electrodes in combination with other ionogel electrolytes. 33,34 In particular, whereas previously reported printed LIBs have typically only been tested at low rates near 0.1C at room temperature, the screen-printed LFP/ LTO full-cells based on the hBN ionogel electrolytes exhibited favorable capacity at higher rates up to 0.5C at room temperature in addition to even higher rate performance up to 2C at 60 °C. Furthermore, the printed LFP/LTO full-cells based on the hBN ionogel electrolytes showed significantly improved cycle life in comparison to previously reported printed LFP/ LTO full-cells. This unprecedented electrochemical performance can be attributed to the high ionic conductivity and electrochemical stability of the hBN ionogel electrolytes.

The mechanically deformable nature of the hBN ionogel electrolytes presents additional opportunities for mechanically

flexible energy storage applications. To demonstrate the mechanical flexibility of the screen-printed LFP/LTO full-cells based on the hBN ionogel electrolytes, bending tests (Figure 4a,b) were performed after the screen-printed LIBs were packaged in sealed plastic bags (Figure S7, Supporting Information). Videos S1 and S2 show the screen-printed LFP/ LTO full-cells during the bending tests, where the screenprinted LIBs were repeatedly bent toward the cathode (Video S1) and anode (Video S2) while being connected to lightemitting diodes (LEDs). Both videos show that the screenprinted LIBs maintain constant power for the LEDs without any observable changes in the LED brightness during repeated bending, thus revealing outstanding bending tolerance regardless of the bending direction. In addition, the bending stability was further confirmed by performing electrochemical impedance spectroscopy analysis during the bending tests. Figure 4c displays Nyquist plots of the screen-printed LIBs before and during bending and also after 200 bending cycles (i.e., 100 bending cycles toward the cathode and 100 bending cycles toward the anode) with a bending radius of 14 mm. The negligible change of the Nyquist plots implies that the hBN ionogel electrolytes allow stable bending deformation without compromising the interfaces between the screen-printed layers.<sup>35</sup> Moreover, the screen-printed LIBs were functional even after folding in half, as shown in Figure S8 (Supporting Information).

In addition to high stability during mechanical deformation, the high mechanical modulus of the hBN ionogel electrolytes provides resilience in the presence of external forces. This attribute is important, since mechanically flexible LIBs are not packaged in hard cases that provide mechanical protection. Furthermore, compared to conventional liquid electrolytes used in combination with membrane separators, the hBN ionogel electrolyte serves as both an ion conductor and a separator. Hence, their mechanical strength is crucial to maintain the separation of the cathode and anode electrodes and thereby avoid short circuits in the presence of external forces. To demonstrate this resilience, pressing tests (Figure 4d) were performed for the screen-printed LFP/LTO full-cells, where compressive forces were applied while the open-circuit voltage (OCV) was monitored (Figure 4e). The compressive forces were gradually raised to 500 N, which corresponds to a pressure of 4.5 MPa with a contact area of 1.1 cm<sup>2</sup>. As shown in Figure 4f, the screen-printed LIBs did not exhibit any signs of failure or significant changes in OCV, implying that the hBN ionogel electrolytes withstood the high pressure and thus inhibited the external forces from forming short circuits between the cathode and anode electrodes. Repeated application of these compressive forces (Figure 4f) also did not result in noticeable changes in OCV, further verifying high resilience against external forces.

The hBN ionogel electrolytes maintain their high mechanical moduli exceeding 1 MPa to temperatures as high as 140  $^{\circ}$ C, as shown in Figure S1 (Supporting Information). This temperature invariance of the hBN ionogel mechanical strength suggests that screen-printed LIBs will retain their outstanding mechanical stability for high-temperature applications. To confirm this high-temperature mechanical stability, pressing tests were repeated while the screen-printed LFP/LTO full-cells were heated, as shown in Figure 4g,h. In this case, a compressive force of 200 N (pressure of 1.8 MPa with a contact area of 1.1 cm²) was applied to the screen-printed LIB on a hot plate at 100  $^{\circ}$ C. Figure 4i displays the resulting charge—discharge voltage profiles at a rate

Nano Letters pubs.acs.org/NanoLett Letter

of 2C, revealing normal LIB operation without voltage instabilities.

In summary, we have developed screen-printable hBN ionogel electrolytes that are suitable for mechanically deformable solidstate LIBs. Screen-printable hBN ionogel electrolyte inks were formulated by mixing solution-exfoliated hBN nanoplatelets, EMIM-TFSI/1 M LiTFSI, and ethyl lactate, resulting in a viscosity of 10 Pa s at a shear rate of 10 s<sup>-1</sup> with shear thinning behavior. These inks enable screen printing of spatially uniform and mechanically flexible hBN ionogel electrolytes that possess high room-temperature ionic conductivities >1 mS cm<sup>-1</sup> and stiff mechanical moduli >1 MPa. Using the hBN ionogel electrolytes, screen-printed LIBs were fabricated with LFP cathode and LTO anode electrodes that exhibited desirable rate performance and cycling stability at both room and elevated temperatures. Furthermore, bending and pressing tests revealed outstanding mechanical resilience of the screen-printed LIBs against bending deformation and external compressive forces, which can be ascribed to the high mechanical flexibility and strength of the hBN ionogel electrolytes. Overall, this work establishes screen-printable hBN ionogel electrolytes as enabling materials for mechanically deformable solid-state LIB technologies.

## ASSOCIATED CONTENT

# **Supporting Information**

The Supporting Information is available free of charge at https://pubs.acs.org/doi/10.1021/acs.nanolett.2c01364.

Viscoelastic properties and ionic conductivity of hBN ionogel electrolytes; viscosity of hBN ionogel electrolyte, LFP cathode, and LTO anode inks; schematic of full-cell assembly; charge—discharge voltage profiles of cycling tests of screen-printed LIBs; photographs of flexible screen-printed LIBs: competitive analysis plot for previously reported printed LIBs using ionogel electrolytes (PDF)

Video S1: Video of bending a screen-printed LFP/LTO full-cell toward the cathode (MP4)

Video S2: Video of bending a screen-printed LFP/LTO full-cell toward the anode (MP4)

# AUTHOR INFORMATION

#### **Corresponding Author**

Mark C. Hersam — Department of Materials Science and Engineering, Department of Chemistry, Department of Medicine, and Department of Electrical and Computer Engineering, Northwestern University, Evanston, Illinois 60208, United States; orcid.org/0000-0003-4120-1426; Email: m-hersam@northwestern.edu

## Authors

Woo Jin Hyun — Department of Materials Science and Engineering, Northwestern University, Evanston, Illinois 60208, United States; Department of Materials Science and Engineering, Guangdong Technion — Israel Institute of Technology, Shantou, Guangdong 515063, China

Cory M. Thomas – Department of Materials Science and Engineering, Northwestern University, Evanston, Illinois 60208, United States

Lindsay E. Chaney – Department of Materials Science and Engineering, Northwestern University, Evanston, Illinois 60208, United States Ana Carolina Mazarin de Moraes — Department of Materials Science and Engineering, Northwestern University, Evanston, Illinois 60208, United States

Complete contact information is available at: https://pubs.acs.org/10.1021/acs.nanolett.2c01364

#### **Author Contributions**

W.J.H. and M.C.H. conceived the idea and designed the experiments. W.J.H., C.M.T., and L.E.C. prepared hBN nanoplatelets. W.J.H. and C.M.T. performed scanning electron microscopy analysis. A.C.M.M. conducted XPS analysis. W.J.H. performed Raman analysis, formulated hBN ionogel electrolyte inks, and characterized the electrochemical and mechanical properties of the hBN ionogel electrolytes. W.J.H. printed and tested batteries. W.J.H. and M.C.H. wrote the manuscript. All authors discussed the results and commented on the manuscript.

#### Notes

The authors declare no competing financial interest.

#### ACKNOWLEDGMENTS

The screen-printable hBN ionogel electrolyte ink development was supported by MilliporeSigma and the U.S. Department of Commerce, National Institute of Standards and Technology (Award 70NANB19H005) as part of the Center for Hierarchical Materials Design (CHiMaD). The solution-based exfoliation of the hBN nanoplatelets was supported by the NSF Future Manufacturing Program (CMMI-2037026). C.M.T. and L.E.C. are supported by the National Science Foundation (NSF) Graduate Research Fellowship under Grant No. DGE-1842165. Scanning electron microscopy and XPS were performed in the NUANCE facility at Northwestern University, which is supported by the Soft and Hybrid Nanotechnology Experimental (SHyNE) Resource (NSF ECCS-1542205), the Materials Research Science and Engineering Center (NSF DMR-1720139), the State of Illinois, and Northwestern University. Rheometry was performed in the MatCI facility, which receives support from the Northwestern University Materials Research Science and Engineering Center (NSF DMR-1720139).

#### REFERENCES

- (1) Tan, D. H. S.; Banerjee, A.; Chen, Z.; Meng, Y. S. From nanoscale interface characterization to sustainable energy storage using all-solid-state batteries. *Nat. Nanotechnol.* **2020**, *15*, 170—180.
- (2) Manthiram, A.; Yu, X.; Wang, S. Lithium battery chemistries enabled by solid-state electrolytes. *Nat. Rev. Mater.* **2017**, *2*, 16103.
- (3) Hyun, W. J.; Thomas, C. M.; Hersam, M. C. Nanocomposite ionogel electrolytes for solid-state rechargeable batteries. *Adv. Energy Mater.* **2020**, *10*, 2002135.
- (4) Chen, N.; Zhang, H.; Li, L.; Chen, R.; Guo, S. Ionogel electrolytes for high-performance lithium batteries: A review. *Adv. Energy Mater.* **2018**, *8*, 1702675.
- (5) Chen, X.; Put, B.; Sagara, A.; Gandrud, K.; Murata, M.; Steele, J. A.; Yabe, H.; Hantschel, T.; Roeffaers, M.; Tomiyama, M.; Arase, H.; Kaneko, Y.; Shimada, M.; Mees, M.; Vereecken, P. M. Silica gel solid nanocomposite electrolytes with interfacial conductivity promotion exceeding the bulk Li-ion conductivity of the ionic liquid electrolyte filler. *Sci. Adv.* **2020**, *6*, eaav3400.
- (6) Hyun, W. J.; Thomas, C. M.; Luu, N. S.; Hersam, M. C. Layered heterostructure ionogel electrolytes for high-performance solid-state lithium-ion batteries. *Adv. Mater.* **2021**, *33*, 2007864.
- (7) Rodrigues, M. T. F.; Kalaga, K.; Gullapalli, H.; Babu, G.; Reddy, A. L. M.; Ajayan, P. M. Hexagonal boron nitride-based electrolyte

- composite for Li-ion battery operation from room temperature to 150 °C. *Adv. Energy Mater.* **2016**, *6*, 1600218.
- (8) Taylor, M. E.; Clarkson, D.; Greenbaum, S. G.; Panzer, M. J. Examining the impact of polyzwitterion chemistry on lithium ion transport in ionogel electrolytes. *ACS Appl. Polym. Mater.* **2021**, 3, 2635–2645.
- (9) Wang, Z.; Tan, R.; Wang, H.; Yang, L.; Hu, J.; Chen, H.; Pan, F. A metal-organic-framework-based electrolyte with nanowetted interfaces for high-energy-density solid-state lithium battery. *Adv. Mater.* **2018**, 30, 1704436.
- (10) Gaikwad, A. M.; Arias, A. C.; Steingart, D. A. Recent progress on printed flexible batteries: Mechanical challenges, printing technologies, and future prospects. *Energy Technol.* **2015**, *3*, 305–328.
- (11) Costa, C.; Gonçalves, R.; Lanceros-Méndez, S. Recent advances and future challenges in printed batteries. *Energy Storage Mater.* **2020**, 28, 216–234.
- (12) Thomas, C. M.; Hyun, W. J.; Huang, H. C.; Zeng, D.; Hersam, M. C. Blade-coatable hexagonal boron nitride ionogel electrolytes for scalable production of lithium metal batteries. *ACS Energy Lett.* **2022**, *7*, 1558–1565.
- (13) Lawes, S.; Sun, Q.; Lushington, A.; Xiao, B.; Liu, Y.; Sun, X. Inkjet-printed silicon as high performance anodes for Li-ion batteries. *Nano Energy* **2017**, *36*, 313–321.
- (14) Gu, Y.; Wu, A.; Sohn, H.; Nicoletti, C.; Iqbal, Z.; Federici, J. F. Fabrication of rechargeable lithium ion batteries using water-based inkjet printed cathodes. *J. Manuf. Process.* **2015**, *20*, 198–205.
- (15) Wei, T. S.; Ahn, B. Y.; Grotto, J.; Lewis, J. A. 3D printing of customized Li-ion batteries with thick electrodes. *Adv. Mater.* **2018**, *30*, 1703027.
- (16) Reyes, C.; Somogyi, R.; Niu, S.; Cruz, M. A.; Yang, F.; Catenacci, M. J.; Rhodes, C. P.; Wiley, B. J. Three-dimensional printing of a complete lithium ion battery with fused filament fabrication. *ACS Appl. Energy Mater.* **2018**, *1*, 5268–5279.
- (17) Deiner, L. J.; Jenkins, T.; Powell, A.; Howell, T.; Rottmayer, M. High capacity rate capable aerosol jet printed Li-ion battery cathode. *Adv. Eng. Mater.* **2019**, *21*, 1801281.
- (18) Sousa, R.; Oliveira, J.; Gören, A.; Miranda, D.; Silva, M. M.; Hilliou, L.; Costa, C.; Lanceros-Mendez, S. High performance screen printable lithium-ion battery cathode ink based on C-LiFePO<sub>4</sub>. *Electrochim. Acta* **2016**, *196*, 92–100.
- (19) Hyun, W. J.; Secor, E. B.; Hersam, M. C.; Frisbie, C. D.; Francis, L. F. High-resolution patterning of graphene by screen printing with a silicon stencil for highly flexible printed electronics. *Adv. Mater.* **2015**, 27, 109–115.
- (20) Ohta, S.; Komagata, S.; Seki, J.; Saeki, T.; Morishita, S.; Asaoka, T. All-solid-state lithium ion battery using garnet-type oxide and Li<sub>3</sub>Bo<sub>3</sub> solid electrolytes fabricated by screen-printing. *J. Power Sources* **2013**, 238, 53–56.
- (21) El Baradai, O.; Beneventi, D.; Alloin, F.; Bultel, Y.; Chaussy, D. Use of cellulose nanofibers as an electrode binder for lithium ion battery screen printing on a paper separator. *Nanomaterials* **2018**, *8*, 982.
- (22) El Baradai, O.; Beneventi, D.; Alloin, F.; Bongiovanni, R.; Bruas-Reverdy, N.; Bultel, Y.; Chaussy, D. Microfibrillated cellulose based ink for eco-sustainable screen printed flexible electrodes in lithium ion batteries. *J. Mater. Sci. Technol.* **2016**, *32*, 566–572.
- (23) Park, M.-S.; Hyun, S.-H.; Nam, S.-C. Mechanical and electrical properties of a LiCoO<sub>2</sub> cathode prepared by screen-printing for a lithium-ion micro-battery. *Electrochim. Acta* **2007**, *52*, 7895–7902.
- (24) Kang, K.-Y.; Lee, Y.-G.; Shin, D. O.; Kim, J.-C.; Kim, K. M. Performance improvements of pouch-type flexible thin-film lithium-ion batteries by modifying sequential screen-printing process. *Electrochim. Acta* **2014**, *138*, 294–301.
- (25) Yu, S.; Mertens, A.; Tempel, H.; Schierholz, R.; Kungl, H.; Eichel, R.-A. Monolithic all-phosphate solid-state lithium-ion battery with improved interfacial compatibility. *ACS Appl. Mater. Interfaces* **2018**, 10, 22264–22277.
- (26) Hyun, W. J.; De Moraes, A. C.; Lim, J.-M.; Downing, J. R.; Park, K.-Y.; Tan, M. T. Z.; Hersam, M. C. High-modulus hexagonal boron

- nitride nanoplatelet gel electrolytes for solid-state rechargeable lithiumion batteries. ACS Nano 2019, 13, 9664—9672.
- (27) Song, L.; Ci, L.; Lu, H.; Sorokin, P. B.; Jin, C.; Ni, J.; Kvashnin, A. G.; Kvashnin, D. G.; Lou, J.; Yakobson, B. I.; Ajayan, P. M. Large scale growth and characterization of atomic hexagonal boron nitride layers. *Nano Lett.* **2010**, *10*, 3209–3215.
- (28) Shi, Y.; Hamsen, C.; Jia, X.; Kim, K. K.; Reina, A.; Hofmann, M.; Hsu, A. L.; Zhang, K.; Li, H.; Juang, Z.-Y.; Dresselhaus, M. S.; Li, L.-J.; Kong, J. Synthesis of few-layer hexagonal boron nitride thin film by chemical vapor deposition. *Nano Lett.* **2010**, *10*, 4134–4139.
- (29) Gorbachev, R. V.; Riaz, I.; Nair, R. R.; Jalil, R.; Britnell, L.; Belle, B. D.; Hill, E. W.; Novoselov, K. S.; Watanabe, K.; Taniguchi, T.; Geim, A. K.; Blake, P. Hunting for monolayer boron nitride: Optical and raman signatures. *Small* **2011**, *7*, 465–468.
- (30) Ye, H.; Lu, T.; Xu, C.; Han, B.; Meng, N.; Xu, L. Liquid-phase exfoliation of hexagonal boron nitride into boron nitride nanosheets in common organic solvents with hyperbranched polyethylene as stabilizer. *Macromol. Chem. Phys.* **2018**, *219*, 1700482.
- (31) Taroni, M.; Breward, C. J. W.; Howell, P. D.; Oliver, J. M.; Young, R. J. S. The screen printing of a power-law fluid. *J. Eng. Math.* **2012**, *73*, 93–119.
- (32) Hyun, W. J.; Lim, S.; Ahn, B. Y.; Lewis, J. A.; Frisbie, C. D.; Francis, L. F. Screen printing of highly loaded silver inks on plastic substrates using silicon stencils. *ACS Appl. Mater. Interfaces* **2015**, *7*, 12619–12624.
- (33) Delannoy, P.-E.; Riou, B.; Lestriez, B.; Guyomard, D.; Brousse, T.; Le Bideau, J. Toward fast and cost-effective ink-jet printing of solid electrolyte for lithium microbatteries. *J. Power Sources* **2015**, 274, 1085–1090.
- (34) Cheng, M.; Jiang, Y.; Yao, W.; Yuan, Y.; Deivanayagam, R.; Foroozan, T.; Huang, Z.; Song, B.; Rojaee, R.; Shokuhfar, T.; Pan, Y.; Lu, J.; Shahbazian-Yassar, R. Elevated-temperature 3D printing of hybrid solid-state electrolyte for Li-ion batteries. *Adv. Mater.* **2018**, *30*, 1800615.
- (35) Gaikwad, A. M.; Chu, H. N.; Qeraj, R.; Zamarayeva, A. M.; Steingart, D. A. Reinforced electrode architecture for a flexible battery with paperlike characteristics. *Energy Technol.* **2013**, *1*, 177–185.